Vaccine 37 (2019) 817–826

Contents lists available at ScienceDirect

Vaccine

journal homepage: www.elsevier.com/locate/vaccine

Needle-free delivery of DNA: Targeting of hemagglutinin to MHC class II molecules protects rhesus macaques against H1N1 influenza

Petra Mooij [a,1], Gunnveig Grødeland [b,*,1], Gerrit Koopman [a], Tor Kristian Andersen [b], Daniella Mortier [a], Ivonne G. Nieuwenhuis [a], Ernst J. Verschoor [a], Zahra Fagrouch [a], Willy M. Bogers [a], Bjarne Bogen [b]

[a] Biomedical Primate Research Centre, Rijswijk, the Netherlands
[b] K.G. Jebsen Centre for Influenza Vaccine Research, Institute of Clinical Medicine, University of Oslo and Oslo University Hospital, N-0027 Oslo, Norway

ARTICLE INFO

Article history:
Received 15 August 2018
Received in revised form 21 December 2018
Accepted 26 December 2018
Available online 9 January 2019

Keywords:
Influenza
DNA vaccine
Antigen presenting cell
APC-targeted antigen
Non-human primates

ABSTRACT

Conventional influenza vaccines are hampered by slow and limited production capabilities, whereas DNA vaccines can be rapidly produced for global coverage in the event of an emerging pandemic. However, a drawback of DNA vaccines is their generally low immunogenicity in non-human primates and humans. We have previously demonstrated that targeting of influenza hemagglutinin to human HLA class II molecules can increase antibody responses in larger animals such as ferrets and pigs. Here, we extend these observations by immunizing non-human primates (rhesus macaques) with a DNA vaccine encoding a bivalent fusion protein that targets influenza virus hemagglutinin (HA) to Mamu class II molecules. Such immunization induced neutralizing antibodies and antigen-specific T cells. The DNA was delivered by pain- and needle-free jet injections intradermally. No adverse effects were observed. Most importantly, the immunized rhesus macaques were protected against a challenge with influenza virus.

1. Introduction

The influenza virus is subject to continuous antigenic drift and more irregular antigenic shifts. Should an antigenic shift produce an influenza virus against which the population is essentially naïve, we may be facing a grave pandemic threat. At present, prophylactic vaccination represents the most effective protective measure against influenza [1]. However, conventional influenza vaccines are hampered by a prolonged production time [2]. In 2009, the conventional influenza vaccine against swine flu was produced in a record-fast production within six months. With this timeline, the vaccine became available only at the same time as the major pandemic wave hit. Thus, novel vaccine formats that can rapidly be produced to prevent an emerging influenza pandemic are greatly needed.

DNA vaccines can be rapidly produced, and as such be tailor-made to efficiently counter newly emerging influenza virus strains. However, DNA vaccines are often poorly immunogenic, underscoring the need to develop more efficient formats. We have developed such an enhancing format by combining DNA delivery with specific targeting of the secreted protein product to antigen presenting cells (APC) [3,4].

Previously, it has been demonstrated that targeting of antigens to antigen presenting cells (APC) increases immunogenicity after immunization [5–7]. Antigens can be coupled to antibodies or natural ligands both by chemical and genetic conjugations, but the resulting protein complexes are often unstable and difficult to produce in sufficient amounts. To remedy these shortcomings, we have developed an APC-targeted vaccine protein format that can be delivered as DNA, and where bivalently displayed antigens are linked via a dimerization unit to MHC class II-specific single chain variable fragment (scFv) targeting units [3]. Using this concept, a single DNA injection was demonstrated to induce strong immune responses in mice, and protection against both tumors [3,8] and influenza virus [4].

A problem with translating this promising DNA vaccination strategy to humans is the extensive polymorphisms of HLA class II molecules. Overcoming this hurdle, we have developed a targeting unit, αpanHLAII scFv, which binds almost all polymorphic HLA-DR and a large fraction of HLA-DQ and HLA-DP molecules [9]. Thus, DNA that expresses the αpanHLAII scFv as targeting unit can most likely be used for vaccination of most if not all humans. A further bonus of the αpanHLAII scFv is that it cross-reacts with MHC class II molecules from several larger mammals, permitting testing of targeted DNA vaccines in these species. Results from vaccination

* Corresponding author.
E-mail address: gunnveig.grodeland@medisin.uio.no (G. Grødeland).
[1] P.M. and G.G. contributed equally to this work.

https://doi.org/10.1016/j.vaccine.2018.12.049
0264-410X/

of ferrets and pigs, using αpanHLAII-targeting of influenza hemagglutinin (HA), demonstrated significantly increased immune responses after a single DNA immunization as compared to non-targeted controls [9].

We here show that the αpanHLAII-specific scFv also cross-reacts with MamuII molecules of rhesus macaques. This is important since that it allows for testing of vaccine efficacy in higher order animals, and thus allow for a closer recapitulation of the immunological events that leads to formation of protective immunity in humans [10,11]. Here, we have immunized monkeys with MamuII-targeted DNA that encode influenza hemagglutinin (HA). The DNA plasmids were deposited in the skin by use of needle-free jet delivery [12–14]. We observed induction of both antigen-specific T cell responses and neutralizing antibodies after immunization, and demonstrated protection against a viral challenge with influenza A/Mexico/InDRE4487/2009 (H1N1) (Mex4487).

2. Materials and methods

2.1. Animals

This study was performed in outbred male, mature, Indian origin rhesus monkeys (*Macaca mulatta)*. Animals were captive-bred for research purposes and socially housed at ABSL-III facilities at the Biomedical Primate Research Center, Rijswijk, The Netherlands (an AAALAC-accredited institution). Animal housing was according to international guidelines for non-human primate care and use (The European Council Directive 86/609/EEC, and Convention ETS 123, including the revised Appendix A as well the 'Standard for humane care and use of Laboratory Animals by Foreign institutions' identification number A5539-01, provided by the Department of Health and Human Services of the United States of America's National Institutes of Health (NIH)). All animal handlings are performed within the Department of Animal Science (ASD) according to Dutch law. ASD is regularly inspected by the responsible authority (Voedsel en Waren Autoriteit, VWA), and by an independent Animal Welfare Officer. The animals were negative for antibodies to simian type D retrovirus, simian T-cell lymphotropic virus, and were selected for absence of antibodies directed to conserved nucleo- and matrix proteins covering all human and avian influenza A and B viruses (Serion ELISA classic Influenza A/B virus IgA/IgG/IgM detection kit (ESR 1231, Serion immunodiagnostica GmbH, Würzburg, Germany)) and to influenza A/PR/8/34 (H1N1) viral lysate (Advanced Biotechnologies Inc, Eldersburg MD, USA). All animals were classified healthy according to physical examination and evaluation of complete blood count and serum chemistry.

Animals were pair-housed with a socially compatible cage mate, and kept on a 12-hour light/dark cycle. The monkeys were offered a daily diet consisting of monkey food pellets, fruit and bread. Enrichment was provided daily in the form of pieces of wood, mirrors, food puzzles, a variety of other homemade or commercially available enrichment products. Drinking water was available *ad libitum* via an automatic watering system. Veterinary staff provided daily health checks before infection, and the animals were checked for appetite, general behavior and stool consistency. During the course of the influenza virus infection the animals were checked twice a day, and scored for clinical symptoms according to a previously published scoring system [15] (skin and fur abnormalities, posture, eye and nasal discharge, sneezing and coughing, respiration rate). A numeric score of 35 or more was predetermined to serve as an endpoint and justification for euthanasia. Each time an animal was sedated the body weight was measured. Body temperature was recorded on a data storage tag (DST, Micro-T, Star-Oddi, Iceland) surgically placed in the abdominal cavity of each animal 28 days before the start of the study, recording body temperature every 15 min. All possible precautions were taken to ensure the welfare and to avoid any discomfort to the animals. All experimental interventions (intra-bronchial infection, swabs, blood samplings, bronchoalveolar lavages) were performed under anesthesia using ketamine (10 mg/kg).

The Institutional Animal Care and Use Committee of the Biomedical Primate Research Centre (dierexperimentencommissie, DEC-BPRC) approved the study protocols developed according to strict international ethical and scientific standards and guidelines. The qualification of the members of this committee, including their independence from a research institute, is requested in the Dutch law on animal Experiments (Wet op de Dierproeven, 1996).

2.2. Vaccination

Animals were randomly distributed to two groups, and immunized with either NaCl (n = 4) or 75 μg DNA encoding αpanHLAII-HA (n = 6) i.d. by Tropis injector (Pharmajet, Colorado, USA), as previously described [9]. The immunization was delivered in 100 μl volumes at two sites 5–8 cm apart on the upper back of the animal, at weeks 0, 6 and 12. The DNA vaccine was prepared with HA (aa 18–541) from influenza A California/07/2009 (H1N1) (Cal07).

2.3. FACS

Rhesus macaque PBMC were incubated with affinity purified αpHLAII-HA proteins [9] (0.5 μg/ml) or non-targeted control proteins (αNIP-HA)[4] for 30 min at 4 °C. Cells were washed (PBS, 1% BSA) and incubated for 30 min at 4 °C with biotinylated anti-human IgG3 (clone HP6017 2 μg/ml, HP6017) (Sigma, MO, USA) in the presence of 1% BSA and 5% human serum. This mAb will detect expression of αNIP-HA and αpHLAII-HA with equal efficiency because the human IgG3 region is included in both constructs. Cells were washed and incubated again for 30 min at 4 °C with a mixture of fluorescently labeled monoclonal antibodies: $CD20^{V450}$ (clone L27), $CD3^{V500}$ (clone SP34), $CD4^{PE\text{-}Cy7}$ (clone SK3), $CD16^{FITC}$ (clone 3G8), $CD123^{PerCP\text{-}Cy5.5}$ (clone 7G3), $HLA\text{-}DR^{APC\text{-}Cy7}$ (clone L243), $CD11c^{AF700}$ (clone S-HCL3) (all from Becton Dickinson, San Jose, Ca, USA), $CD8^{BV570}$ (RPA-T8, Biolegend, San Diego, CA, USA), $CD14^{ECD}$ (clone RM052, Beckman Coulter, Brea, CA, USA), $CD1c^{APC}$ (clone AD58E7, Miltenyi Biotec GmbH, Bergisch Gladbach, Germany), and SAV^{PE} (DAKO, Glostrup, Denmark). Samples were run on FACSaria (BD Biosciences, NJ, US), and analyzed using FlowJo Software (Version 7.6) (FlowJo, OR, US). To analyze the binding of the HA constructs to different cell subsets the following gating strategy was used (see Fig. S1): an extended lymphocyte gate was drawn to include lymphocytes as well as monocytes and DC. Subsequently, CD3 was plotted against HLA-DR, and T cells (CD3+/HLA-DR-) were selected. The CD3-/HLA-DR+population was further analyzed by plotting CD14 against CD20 and B cells (CD14-/CD20+), and monocytes (CD14-/CD20+) were selected. CD14-/CD20- cells were selected to define CD11c+/CD123- mDC as well as CD11-/CD123+pDC subsets. NK cells were defined as CD3-/HLA-DR-/CD16+.

2.4. Serum ELISA

Serum samples were tested for the presence of anti-influenza virus antibodies using ELISA, as previously described [16]. Briefly, 96-well microtiter plates (Nunc Maxisorp, Sigma Aldrich, MO, US) were coated with Pandemrix [1:100, antigen suspension with A/California/7/2009 (H1N1)-like strain (X-179A)] (Glaxo Smith Kline, UK), blocked (PBS with 1% BSA), and diluted serum samples added. Bound anti-HA antibodies were detected using alkaline phosphatase-conjugated Protein G (1:1000 diluted in PBS)

(Calbiochem EMD Millipore Corporation, US), and plates developed with BluePhos Microwell Phosphatase Substrate System (KPL, Kirkegaard & Perry Laboratories, US). The absorbance was measured at 595 nm.

2.5. Microneutralization assay

Microneutralization assay was performed as previously described, but in the absence of TPCK trypsin [4]. Briefly, two-fold serial dilutions of heat inactivated serum samples were incubated in duplicates for 2 h at 37° C and 5% CO_2, with 100 $TCID_{50}$ influenza A H1N1 (Mex4487). Next, 1.5×10^4 MDCK cells were added to each well, and plates incubated overnight at 37 °C, 5% CO_2. Plates were washed and cells fixed in cold 80% acetone. Then, plates were air-dried, and viral proteins detected with ELISA using anti-nucleoprotein (NP) mAb (H16-L10-4R5, HB65) (1:1000, ATCC, VA, US) and goat anti-mouse HRP antibody (1:2000) (KPL, Gaithesburg, MD, USA). The reaction was developed with OPD (o-phenylenediamine dihydrochloride) (Sigma Aldrich, MO, US) and stopped with sulphuric acid. Absorbance was measured at 490 nm. Neutralization titers were determined by the reciprocal serum dilution giving more than 50% OD reduction.

2.6. Haemagglutination inhibition assay (HAI)

HAI assays were performed on serum samples as previously described [16]. Briefly, non-specific inhibitors were removed by treatment of serum samples with RDE (receptor destroying enzymes), and then incubated for 1 h with 50% Turkeys Red Blood Cells (TRBC) in PBS. HAI assays were performed by standard procedures in 96-well V-bottom microtiter plates (Greiner, Sigma-Aldrich, MO, US) using 0.5% TRBC. Two-fold serial dilutions of sera were made from a starting dilution of 1:10 to 1:5120 in PBS solution. The serum dilutions were incubated with 0.5% TRBC for 45 min at room temperature, and agglutination determined by visual inspection. Titers were expressed as the reciprocal of the highest dilution of plasma that completely inhibited 8 haemagglutinating units of Mex4487 influenza virus. Samples were tested in duplicate.

2.7. IFNγ ELISPOT assay

ELISpot assay was performed with samples in triplicates according to the manufacturer's protocol (U-CyTech biosciences, Utrecht, The Netherlands). In brief, $1{,}2 \times 10^6$ freshly isolated PBMCs were stimulated for 16 h with 5 μg/ml rec. HA from A/California/07/2009 (H1N1) (Sino Biologicals, PA, US) in a 48-well tissue culture plate (Becton Dickinson, NJ, US). After stimulation, non-adherent cells were collected with pre-warmed RPMI-1640 medium, and plated out (2×10^5 cells/well) in PVDF ELISpot plates (Millipore, MA, US) (including stimulus of 5 μg/ml rec. HA), that previously had been activated with 35% ethanol (15 μl/well) for one minute, coated ON with anti-IFN-γ mAb MD-1 (U-CyTech) and blocked ON with blocking buffer. The negative control was medium alone, the positive control a PMA/ionomycin mixture (used at 20 ng/ml and 1 μg/ml respectively). Cells were then incubated for 4 h at 37 °C, 5% CO_2, and spots detected with biotinylated rabbit-anti-rhesus IFN-γ mAb (U-CyTech) and streptavidin-HRP (RPN1231V, GE Healthcare, Buckinghamshire) on an AEC (3-amino-9-ethylcarbazole) colouring system. Spots were automatically counted using A.EL.VIS ELISpot reader (A.EL.VIS, Hannover, Germany).

2.8. Intracellular cytokine staining (ICS)

ICS was performed on cells present in BAL fluid collected at day 14 after influenza infection. Cells were incubated at 37 °C for 2 h with anti-CD49d (clone L25, BD Pharmingen, San Diego, CA) and ECD labelled anti-CD28 (CD28.2, Beckman Coulter, Los Angeles, CA) antibodies (1 μg/ml of each antibody), and either staphylococcal enterotoxin B (1.25 μg/ml; Sigma, St. Louis, MO), HA protein (5 μg/ml) or medium only. Then, brefeldin A (Golgiplug 1:1000, BD Pharmingen) was added to inhibit protein trafficking, and cells were incubated further for 12 h at 37 ℃. Cells were then washed with PBS and incubated with 50 μl of live/dead fixable violet dead cell stain kit (Molecular Probes, cat. no. L34955) diluted in PBS for 15 min at 4 ℃ in the dark. Next, cells were stained for surface markers by adding 50 μl PBS/1% BSA containing a mixture of $CD8^{V500}$ (clone SK1), $CD3^{BV650}$ (clone SP34.2), $CD4^{PerCP\text{-}Cy5.5}$ (clone L200), $CD95^{FITC}$ (clone DX2) (all from BD Pharmingen), and incubated for 15 min. at 4 ℃ in the dark. Then all samples were washed with PBS/BSA and fixed with cytofix/cytoperm solution (BD Pharmingen) for 20 min at 4 °C. Subsequently, the cells were washed with permeabilization buffer (diluted 10x in H2O) and resuspended in permeabilization buffer containing 5% normal human serum (Sanquin, Amsterdam, The Netherlands), anti-$CD69^{APC\text{-}H7}$ (clone FN50), anti-$IL2^{PE}$ (clone MQ1-17H12), anti-$TNF\alpha^{PE\text{-}Cy7}$ (clone Mab 11) and anti-$IFN\gamma^{Alexa700}$ mAb (clone B27, all from BD Pharmingen). After 30 min. incubation at 4 °C, cells were washed twice with permeabilization buffer and fixed in 2% paraformaldehyde solution (in PBS) for 16 h. Acquisition was performed on a LSRII flow cytometer.

2.9. Virus

A/Mexico/InDRE4487/2009 (H1N1) (Mex4487) was originally isolated from the bronchial aspirate of a 26-year-old man from a family cluster of three confirmed severe flu cases in Mexico [15]. The virus was kindly provided by Dr. Y. Li and Dr. G. Kobinger from the Public Health Agency of Canada, National Microbiology Laboratory, Canadian Science Centre for Human and Animal Health, Winnipeg, MB, Canada, and propagated on MDCK cells. $TCID_{50}$ was determined.

2.10. Experimental infection and influenza virus detection

Rhesus macaques were experimentally inoculated four weeks post the final immunization with 4×10^7 $TCID_{50}$ of influenza Mex4487. Infection was performed as previously described [17], via the intra-bronchial route using a bronchoscope, with a total of 4 ml virus suspension containing 10^7 $TCID_{50}$/ml split into 2 ml doses, one per bronchus. During the infection procedure, animals were sedated with ketamin (10 mg/kg) and medetomidine hydrochoride (0.04 mg/kg, Cepetor), and local anesthesia in the throat applied by spraying with 10% Xylocain (Lidocain). At the end of the procedure, Atipamezol hydrochloride, 0.5 mg/kg (Revertor) was used for faster recovery. Tracheal swabs were collected before and 1, 2, 4, 6, 8, 10, 14 and 21 days post infection using Copan flocked swabs (FLOQswabs, 502CS01, COPAN, Italy). BAL fluid was collected at day 6 and 14 post infection using a bronchoscope. Viral RNA was isolated using a QIAamp Viral RNA Mini kit (Qiagen Benelux BV, Venlo, The Netherlands) following the manufacturer's instructions and was detected by real-time PCR [18].

2.11. Assessment of cytokine and chemokine protein levels in serum

Cytokine and chemokine concentrations, including G-CSF, GM-CSF, IFNγ, IL-1β, IL-1Ra, IL-2, IL-4, IL-5, IL-6, IL-8, IL-12, IL-13, IL-15, IL-17a, IL-18, MCP-1, MIP-1α, MIP-1β, sCD40L, TGFα, TNFα, VEGF, were determined using the MILLIPLEX MAP Non-Human Primate Cytokine Magnetic Bead Panel kit (Millipore, Billerica, MA, USA) and a Luminex detection system (Luminex Corporation, Austin, USA), according to the manufacturer's instructions. For each cytokine a standard curve was made, ranging from 2.4 to

10,000 pg/ml. Samples were measured on a Bio-Plex 2000 system (Bio-Rad, Herts, UK) and analyzed by using Bio-Plex Manager software.

2.12. Statistical evaluation

Statistical significance of differences between the dose groups was calculated by using the Mann-Whitney test. A two-sided α level of 0.05 was used to determine significance.

3. Results

3.1. Binding of MHCII-targeted vaccines to rhesus macaque APC

We have constructed vaccine plasmids encoding a vaccine format where influenza hemagglutinin (HA) from influenza virus A/California/07/2009 (H1N1) is targeted to human HLAII-molecules, via a dimerization unit consisting of the hinge and C_H3 domain of human γ3 Ig H chains. The targeting unit was demonstrated to broadly bind human HLA class II molecules, and also to cross react with MHC class II molecules of horses, cows, pigs and ferrets [9]. Here, we assessed the ability of this panMHCII-specific vaccine, denoted αpHLAII-HA, to bind rhesus macaque leucocytes from four different individuals. The binding profile of αpHLAII-HA was compared to a non-targeted control, where the αpHLAII-targeting unit was replaced with a scFv specific for the hapten NIP (αNIP-HA)[4] (non-targeted control). We found that the αpHLAII-directed targeting unit preferentially bound APC with high expression of Mamu class II molecules, such as B cells, monocytes, myeloid and plasmacytoid dendritic cells (DC) (Fig. 1 and S1B). Binding to T cells and NK cells was much weaker, consistent with a lower display of MHC class II molecules on these cell types. Essentially identical results were obtained in four different individuals.

3.2. Jet delivery of DNA vaccines induces strong antibody responses in rhesus macaques

Rhesus macaques were immunized thrice with plasmids encoding αpHLAII-HA or mock-immunized with NaCl, and post-immunization sera examined for induction of HA-specific antibodies. While the first DNA immunization only raised sporadic antibody responses, the second immunization induced good antibody titers in four out of the six monkeys immunized with αpHLAII-HA (Fig. 2A). The third DNA vaccination further boosted these antibody titers, and all monkeys responded ($p < 0.01$, Mann Whitney test). No adverse effects were observed after the vaccinations.

For a more qualitative assessment of antibody responses, sera collected at week 14 were examined in a microneutralization assay and a haemagglutination inhibition assay (HAI) with influenza virus A/Mexico/InDRE4487/2009 (H1N1) (Mex4487) (Fig. 2B). The levels of neutralizing anti-HA antibodies ranged from titers of 40 to 320 in the monkeys vaccinated with αpHLAII-HA, in contrast to the NaCl-vaccinated group ($p = 0.0313$). The HAI titers were much lower, reaching only a maximum of 40, and were detectable in five of the six vaccinated, but in none of the control animals ($p = 0.033$).

3.3. T-cell responses induced after DNA vaccination

A single DNA immunization induced HA-specific IFNγ T cell responses in 2 out of 6 rhesus macaques (R4 and R5) immunized with αpHLAII-HA. After the second immunization, T cell responses were enhanced in all animals in this group (Fig. 2C). The responses went down after the third immunization, except in two monkeys where the responses stabilized (R5) or continued to increase (R4). These two monkeys were later the ones that were protected against an influenza virus infection (Fig. 3A). As expected, none of the monkeys that received NaCl showed an increase in HA-specific T cell responses, and responses were significantly higher in αpHLAII-HA vaccinated animals two weeks after the second and third immunization (week 8 and 14, $p < 0.01$ Mann-Whitney test) (Fig. 2C). Notwithstanding these clear results, it must be noted that the number of Spot Forming Units (SFU) was rather low and ICS analysis was not pursued because of the generally lower sensitivity of this assay.

3.4. DNA immunizations protect rhesus macaques from pandemic H1N1 infection

Four weeks after the third immunization (week 16), all animals received influenza virus Mex4487 via the intra-bronchial route. Throughout the post infection phase, tracheal swabs were collected to monitor development of the influenza virus infection by real-time PCR. Results showed that virus was never detected in 2/6 monkeys (R4 and R5) immunized with αpHLAII-HA, and only at one time point in two other monkeys (R2 and R3) (Fig. 3A). By contrast, all macaques in the NaCl group had high concentrations of virus in tracheal swabs. These results demonstrate that the viral load was significantly reduced in monkeys receiving αpHLAII-HA, as compared to the NaCl group (Fig. 3B), $p = 0.01$.

At day 6, broncho-alveolar lavage fluid (BAL) was collected as an additional read-out of infection (Fig. 3C). Analyses of viral titers confirmed that infection was significantly reduced in the group that received the αpanHLAII-HA vaccine, as compared to the NaCl group ($p < 0.01$). By day 14, the virus was cleared from all animals, including the NaCl group. When comparing the data from tracheal swabs and BAL, it is noteworthy that the αpHLAII-HA-immunized animals that did not show influenza virus in tracheal swabs (R4 and R5), were also negative for virus in BAL.

During the course of the influenza infection, the body temperature of individual animals was recorded every 15 min on a data logger that was surgically placed in the abdominal cavity. Prior to infection, a reference 24-hour body temperature cycle was constructed for each animal using the 7-day period just before infection. Each animal showed a clear circadian body temperature pattern, with lowest temperatures around midnight and highest around 15:00 in the afternoon (Fig. S2). The net increase in body temperature during the 21-day post challenge period was calculated as difference relative to the upper 95% confidence limit of the reference cycle at corresponding times [16,17]. The lower limit of the temperature difference was set at zero to reduce the impact of lower body temperatures during post challenge anesthesia. Unfortunately, temperature was not recorded in animal R9 (NaCl group), due to data logger failure.

Monkeys treated with NaCl showed two fever peaks, at 1–2 days and 6–7 days after influenza virus infection (Fig. S2, B). The second fever peak was not observed in monkeys immunized with αpHLAII-HA (Fig. S2, A). In addition, the total AUC of the body temperature net increase was lower in 5 out of 6 animals immunized with αpHLAII-HA, as compared to NaCl animals (Fig. 3 D). Clinical signs, such as skin and fur abnormalities, hunched posture, eye and nasal discharge, sneezing and coughing, increased respiration rate, changes in stool consistency, loss of appetite, and lethargy are hardly ever seen after influenza virus infection, and, as expected, no differences were observed between immunized and control animals.

We also measured anti-HA antibodies 4 weeks after viral challenge. While all animals had strongly increased antibody titers of anti-HA IgG, the anti-HA antibody levels were significantly higher in αpHLAII-HA than in the NaCl group (Fig. 3E, $p < 0.01$,

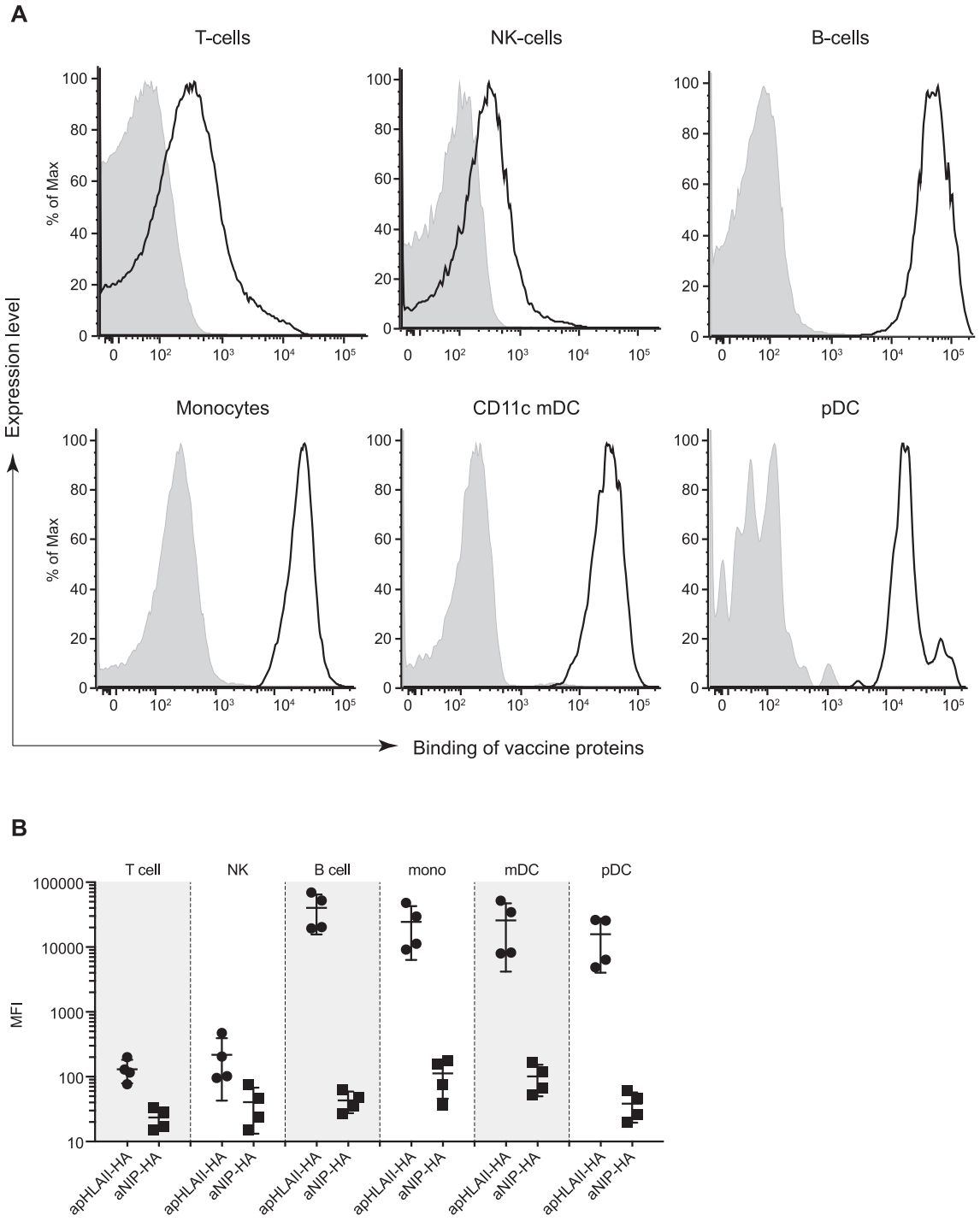

Fig. 1. Characterization of vaccine protein binding. PBMC from rhesus macaques (n = 4) were incubated with purified αpHLAII-HA (line) or non-targeted control (αNIP-HA) (grey area), and binding to gated immune cells was evaluated. (A) Representative example (animal R04086) showing expression profiles in different leukocyte subsets. (B) Strength of fluorescent signal observed in T cells, NK cells, B cells, monocytes, mDC and pDC after incubation of PBMC with αpHLAII-HA versus αNIP-HA. mDC: myeloid dendritic cells, pDC: plasmacytoid dendritic cells, MFI; mean fluorescence intensity.

Mann-Whitney test). The fact that all monkeys had increased antibody titers, including the animals that remained virus negative throughout the study period (animals R4 and R5), argues that the viral challenge was effective for all animals.

In order to study whether the experimental infection also resulted in higher cellular immune responses in the group vaccinated with αpHLAII-HA as compared to the NaCl group, an ICS assay was performed on cells present in BAL samples taken at day 14 after infection. As shown in Fig. 4, the CD4 responses against HA protein were significantly higher for αpHLAII-HA than the NaCl group ($p = 0.01$). The CD8 responses were lower, and no significant differences were observed between the vaccine and the control group. A large majority of the cytokine producing cells observed were polyfunctional, expressing IFNγ, IL2 and TNFα. Strikingly, the two protected animals (R4 and R5) had the highest CD4 responses.

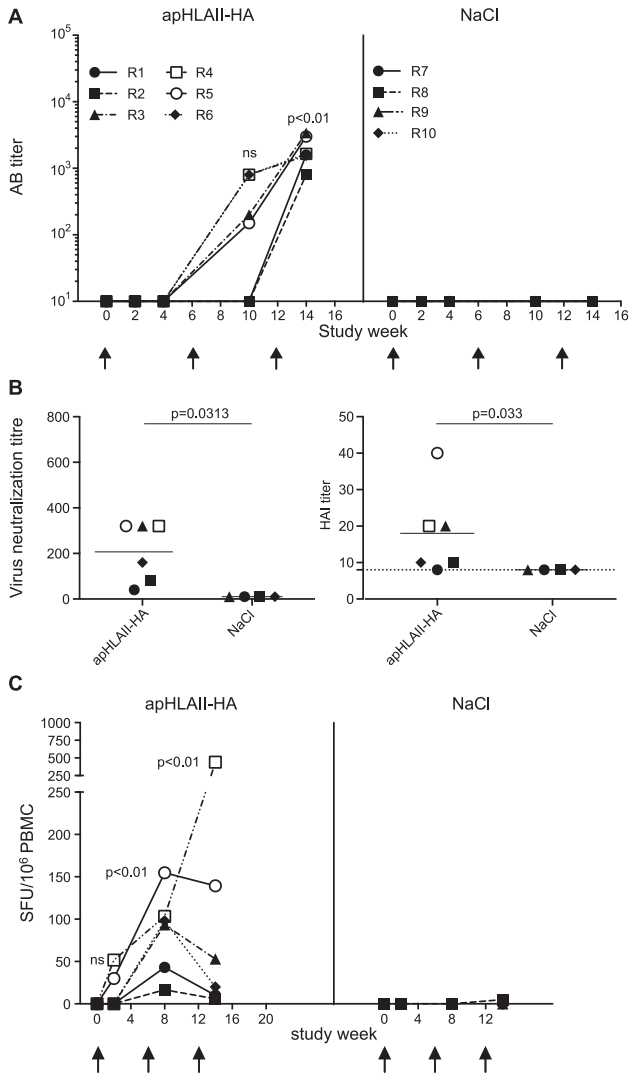

Fig. 2. Immune responses after vaccination. Rhesus macaques were vaccinated with 75 μg of DNA plasmids encoding the indicated vaccines, delivered i.d. at weeks 0, 6 and 12 with jet delivery. (A) Sera were harvested at weeks 0, 2, 4, 10 and 14, and the development of IgG responses against influenza H1N1 (Cal07) measured in individual animals (R1-R10) by ELISA. Arrows indicate time points of immunizations. (B) Sera harvested at week 14 were assessed for neutralizing antibodies (left graph) and HAI (right graph) against A/Mexico/InDRE4487/2009 (H1N1) (Mex4487). Depicted is the reciprocal of the serum dilution giving 50% influenza virus reduction. The lowest serum dilution tested in the HAI assay was 1:10. Samples that were negative at 1:10 dilution are plotted on the stippled horizontal line. (C) PBMC harvested at weeks 0, 2, 8 and 14 were stimulated with recombinant HA protein (Cal07), and evaluated for induction of HA-specific IFNγ-secreting T cells by ELISpot assay. The numbers of spot forming units (SFU)/10^6 PBMC are depicted. (A-C) Significant differences were evaluated with the Mann-Whitney test.

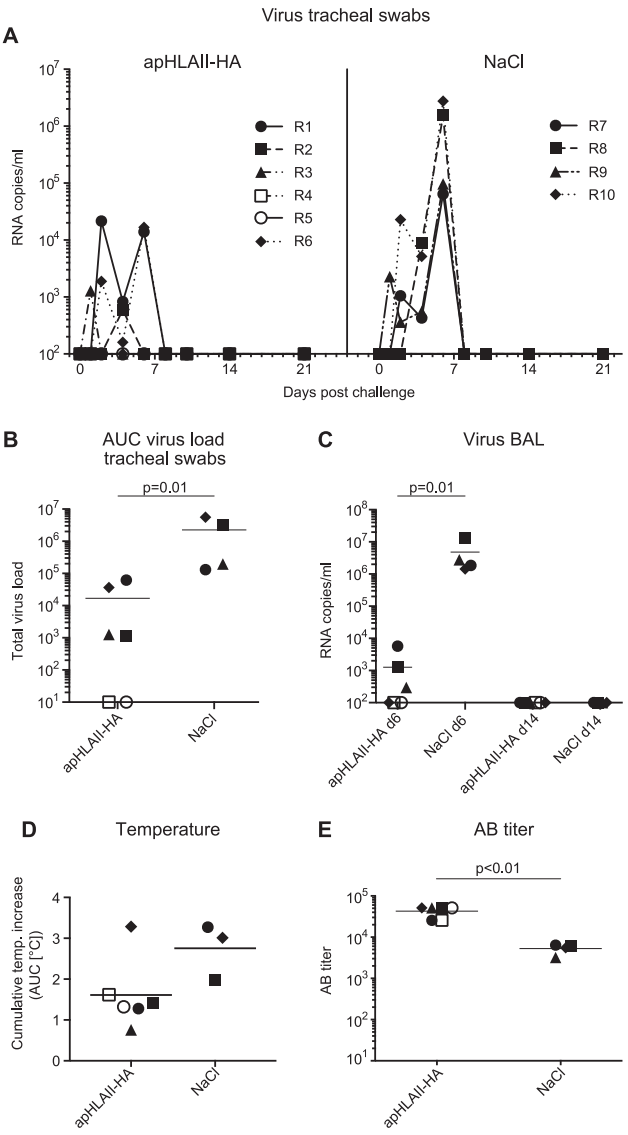

Fig. 3. Influenza viral load, body temperature, and antibody responses after challenge with A/Mexico/InDRE4487/2009 (H1N1) (Mex4487). (A) Tracheal swabs were collected regularly starting from the day of viral challenge (days 0, 1, 2, 4, 6, 8, 10, 14 and 21), and assayed for viral load by QRTPCR. (B) Summary of the total virus load day 0–21 post infection, measured as area under the curve (AUC). (C) Broncho alveolar lavage fluids (BAL) were collected at days 6 and 14 post infection, and viral load measured by QRTPCR. (D) Body temperature increase (in °C) calculated as area under the curve (AUC) from continuously recorded body temperatures during 21 days after influenza virus infection, minus the mean circadian body temperature pattern recorded before infection. Due to data logger failure, body temperatures of animal R9 (NaCl) were not recorded. See Fig. S2 for details from individual animals. (E) Sera were harvested from individual animals at 4 weeks post challenge, and tested for IgG responses against influenza H1N1 (Cal07) by ELISA. (B-E) Statistical differences between groups were determined with Mann-Whitney test.

3.5. Jet delivery of DNA reduced peak cytokine and chemokine levels after influenza virus infection

Influenza infection triggers the development of particular cytokines and chemokines [19]. Thus, we have assessed the expression of 22 different cytokines and chemokines in sera after influenza infection (Fig. 5, and Supplemental Table 1). Interestingly, the profiles of IL-6, MCP-1 and IFNγ in sera were different between the αpHLAII-HA vaccinated group and NaCl treated animals. For all these molecules, we observed a sharp increase after infection in monkeys sham-immunized with NaCl. In contrast, IL6 was barely detectable in αpHLAII-HA immunized monkeys (Fig. 5A), and only minimal increases of MCP-1 were observed in this group (Fig. 5B).

The peak IL-6 levels at day 1 post-infection were also significantly higher in NaCl animals than in αpHLAII-HA-immunized monkeys (Fig. 5A, right panel), while the difference in MCP-1 did not reach statistical significance (Fig. 5B). Noteworthy, the protected animals (R4 and R5, open symbols in Figures) did not show an increase in any of these cytokines after influenza virus challenge. The levels of IL-15 peaked in all the infected monkeys around days 1–2, but then a more rapid decrease was observed in the monkeys immunized with αpHLAII-HA, as opposed to NaCl immunization (Fig. 5D). The increase in IFNγ levels seems to occur in two phases roughly corresponding to the fever peaks (Fig. S2) in monkeys sham-immunized with NaCl (Fig. 5C). The second peak levels of

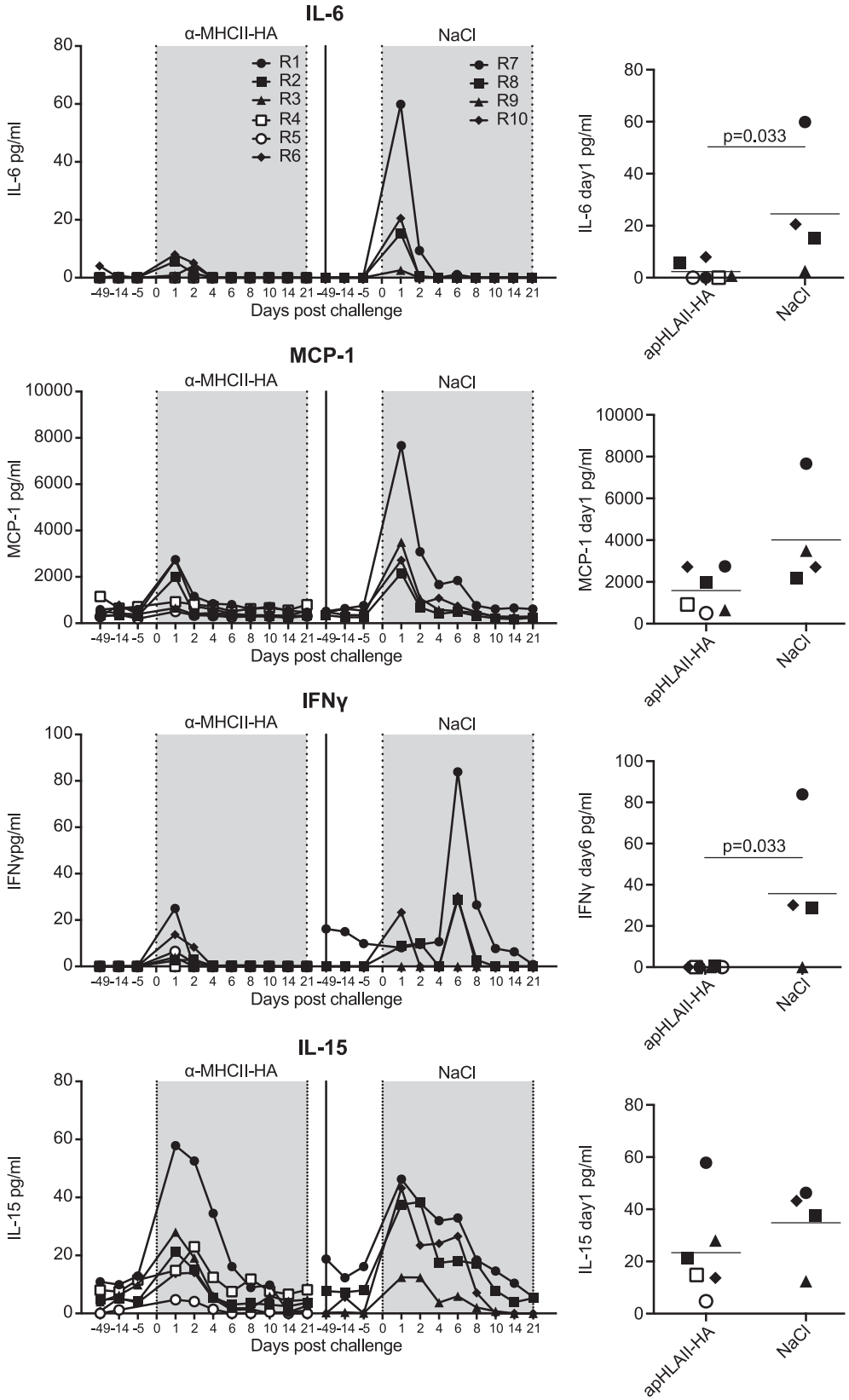

Fig. 4. Antigen specific cytokine responses measured by ICS in BAL post-infection. (A) Percentage of HA-specific $CD4^+$ and $CD8^+$ T cells expressing cytokines (IFNγ, IL-2, TNFα) in BAL collected at day 14 after influenza virus infection. (B) Cytokine expression pattern of HA-specific responses in $CD4^+$ and $CD8^+$ T-cells. Pies indicate the relative number of cells expressing one (dark blue), two (yellow) or three (orange) cytokines. Arcs indicate production of IFN-γ (red), IL-2 (green) and TNF-α (blue). (For interpretation of the references to colour in this figure legend, the reader is referred to the web version of this article.)

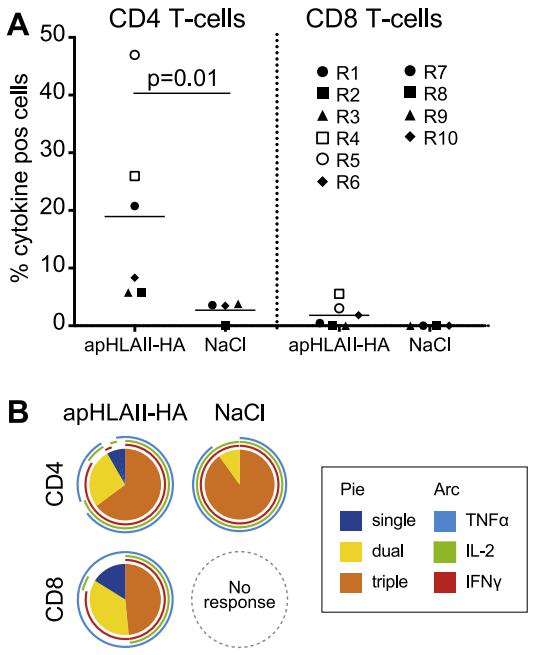

Fig. 5. Cytokine and chemokine expression levels in sera. Sera were harvested at various time points prior to, and after, influenza virus challenge. Day 0 represents the day of challenge, and days 0–21 after infection are shaded in grey for clarity. The individual panels show amounts of (A) IL-6, (B) MCP-1, (C) IFNγ, and (D) IL-15 measured as pg/ml in serum over time. Statistical differences at peak levels (at day 1 for IL-6, MCP-1, and IL-15, and at day 6 for IFNγ) between groups were determined with Mann-Whitney test and are depicted in the graphs on the right.

IFNγ at day 6 were not observed in αpHLAII-HA immunized animals (and there was also no second fever peak in these animals, S2), but only in the control NaCl monkeys (Fig. 5C, right graph). Although the control monkey R7, that had the highest IFNγ peak after infection, already showed higher IFNγ levels before influenza infection than all other animals, it did also show the same kinetics profile in cytokine increase as all other animals, and can therefore not be considered as an outlier.

4. Discussion

Rapid availability of relevant influenza vaccines is important in response to an emerging influenza pandemic. Where current formats for influenza vaccines require a prolonged and cumbersome production, DNA vaccines can be quickly produced within 2–3 months. Furthermore, DNA is relatively stable at room temperature and can be distributed globally independent of a cold chain. Here, we have demonstrated that a DNA vaccine, delivered into the skin with a needle free device, can protect rhesus macaques against an infection with H1N1 influenza virus (Mex4487). This is important since DNA vaccines can be rapidly modified to accommodate HA from a newly emerged strain of influenza virus, and as such contribute the needed protection in the event of a threatening influenza pandemic.

The rationale behind the present vaccination strategy is to let the DNA encode a bivalent fusion protein that, subsequent to secretion from transfected cells, targets MHC class II surface molecules for delivery of antigen. In previous experiments in mice [4], ferrets and pigs [9], this strategy has resulted in increased antibody and T cell responses compared to non-targeted versions of the vaccine molecule or antigen alone. Moreover, a single immunization sufficed to elicit protective antibody responses. In the study presented here, we observed that rhesus macaques needed a booster delivery of αpanHLAII-HA for antibody responses to be observed. There may be several explanations for this; (i) Several non-professional APCs in rhesus macaques also express MHCII molecules. Examples are keratinocytes [20–22], natural killer cells [23], and T cells [24]. It is possible that binding of MHCII-targeted vaccines to these cells will absorb vaccine proteins that could otherwise have been available for activation of professional APC. (ii) Targeting of antigen to MHCII in rhesus macaques may be mechanistically different from other species. Whilst the αMHCII-specific scFv bound APC in 4/4 rhesus macaques (Fig. 1), and humans and rhesus monkeys share most of the MHC class II loci (including HLA-DR, -DP, and –DQ)[25], rhesus macaques have more complex polymorphisms in the class I and class II loci [26] that could influence antigen presentation [27]. Importantly, we have in neither rhesus macaques, pigs, nor ferrets, observed adverse effects following MHCII-targeted vaccination, and also in all species demonstrated induction of neutralizing antibodies following MHCII-targeted vaccination. It is encouraging that DNA vaccination in rhesus macaques with αpHLAII-HA resulted in induction of both antibodies and T cell responses, reduction in viral loads upon challenge, and reduction of fever. Thus, DNA immunization with needle-free jet delivery should clearly be pursued also in humans.

Vaccination with αpHLAII-HA induced IFNγ-secreting T cells in 2/6 animals after a single vaccination, and in 6/6 after the second (Fig. 2C). The two early responders (R4 and R5), also showed the highest T-cell response after the final boost and were the same monkeys that were protected from influenza virus infection. R4 and R5 also showed high neutralizing antibodies titers, as did R3. It is therefore likely not neutralizing antibodies alone that protected them, since monkey R3, R4 and R5 had the same neutralizing antibody titres, but monkey R3 got infected. Conversely, R4 and R5 that were completely protected had the highest T cell responses (ELISPOT) after the 3rd immunization compared to any of the other monkeys, including R3. It therefore appears as though a combination of both high virus neutralizing antibodies and robust T cell responses are required for sterilizing immunity. Since the sensitive ELISPOT technique used here did not distinguish between CD4 and CD8 T-cells, we cannot conclude whether the T-cell response in R4 and R5 are only CD4 T cells that help stimulating the B cell antibody induction, or if any cytotoxic CD8 T cells were involved in the protective mechanism. This could have been studied with intracellular cytokine staining (ICS) and FACS analysis, but the ELISPOT responses were still relatively modest and with the less sensitive ICS method most probably not detectable. Instead we used ICS to assess whether a difference could be observed between the vaccine and control group after viral challenge. Indeed, strong CD4 T-cell responses were observed in BAL samples taken at day 14 after infection in the αpHLAII-HA vaccine group. These responses were significantly higher than in the NaCl group, and the protected animals R4 and R5 again were the highest responsers. These data confirm the pre-challenge ELISpot and ELISA data, and indicate that the vaccine effect translates to induction of high responses in the lung after subsequent infection.

While T cells alone cannot confer sterilizing immunity against influenza, they can often mediate broader protection against different strains or subtypes of influenza. As such, the T cells induced after MHCII-targeted vaccination could potentially confer protection against influenza strains that have evolved beyond antibody recognition. If one would like to further optimize T cell reactivity, we have previously demonstrated in mice that chemokine receptor targeting with MIP1-α [28] and Xcl1 [29] is particularly efficient for improved T cell responses. Thus, for elicitation of improved T cell responses against influenza antigens in rhesus macaques, chemokine targeting units (MIP1-α, Xcl1) should be tested as APC-targeted DNA vaccines.

Upon vaccination in pigs with targeted DNA vaccines, delivery with either electroporation or jet delivery gave similar results [9].

Since jet delivery is needle-free and apparently pain-free, and thus attractive for human application, we chose to use jet delivery in the present experiments. Previous studies in rhesus macaques have demonstrated that genetic vaccines given either in combination with electroporation or by gene gun administration are immunogenic [30,31], and can achieve a reduction in viral shedding upon experimental viral challenge [32,33]. That said, most of these vaccines included in addition to HA other influenza virus proteins (such as nucleoprotein or the ion channel protein M2), and these may have contributed to the observed outcomes [32]. Further, we do not know how jet delivery of DNA compares with delivery by electroporation or gene gun in rhesus macaques. Also, while electroporation has been shown to have an adjuvant effect at least in mice [34], this is not known for jet delivery. Presumably, jet delivery increases uptake of plasmids in skin cells, resulting in increased secretion of bivalent vaccine proteins that target $MHCII^{POS}$ APC. What type of dermal cells that become transfected with plasmids, is not known. Also, it is unknown whether vaccine proteins drain via afferent lymphatics to lymph nodes and prime APC in this location, or whether APC in skin are primed, followed by migration to lymph nodes. Experiments with injection of αMHCII-targeted plasmids into mouse muscle, combined with electroporation, indicate that a local inflammation may be ensued by infiltration of $MHCII^{POS}$ APC around transfected muscle cells [35]. However, a major part of the immune response elicited by targeted DNA vaccines is likely to take part in draining lymph nodes where primed APC and stimulation of T cells can be detected [8].

In summary we have shown that jet delivery of DNA and targeting of HA to MHC class II molecules protect Rhesus macaques against H1N1 influenza virus infection. This type of needle free DNA vaccination may, with improvements, become an effective way to rapidly and efficiently protect individuals against emerging seasonal or pandemic influenza virus strains.

Acknowledgments

We thank Pharmajet Inc. for providing the apparatus for jet injections, and Dr. Y. Li and Dr. G. Kobinger from the Public Health Agency of Canada, National Microbiology Laboratory, Canadian Science Centre for Human and Animal Health, Winnipeg, MB, Canada for providing the influenza A/Mexico/InDRE4487/2009 (H1N1) (Mex4487) virus. The technical help of H. Niphuis, Dr. I. Kondova, A.G.M. Haaksma, Dr. G Doxiadis, and F. van Hassel (all from the Biomedical Primate Research Center, Rijswijk, The Netherlands), is gratefully acknowledged. This study was funded by the K.G. Jebsen Foundation, Norway, the Biomedical Primate Research Center, Rijswijk, The Netherlands, and part of this work has been supported by EUPRIM-Net under the EU contract 262443 of the 7th Framework Programme. The funders had no role in study design, data collection and interpretation, or the decision to submit the work for publication.

Competing interests

BB and GG are inventors on patent applications filed on the vaccine molecules by the TTO offices of the University of Oslo and Oslo University Hospital, according to institutional rules. BB is head of the Scientific panel of Vaccibody AS, and hold shares in the company.

Author contributions

GG, PM, GK, BB and WB conceived and designed experiments. PM, GK, GG, TKA, DM, IN, EV, and ZF performed experiments, PM, GK, GG and BB analyzed experiments. GG, GK, PM and BB wrote the paper, but all authors commented and edited on the paper.

Appendix A. Supplementary material

Supplementary data to this article can be found online at https://doi.org/10.1016/j.vaccine.2018.12.049.

References

[1] Dominguez A, Godoy P, Torner N. The effectiveness of influenza vaccination in different groups. Expert. Rev. Vacc. 2016:1–14.
[2] Osterholm MT, Kelley NS, Sommer A, Belongia EA. Efficacy and effectiveness of influenza vaccines: a systematic review and meta-analysis. Lancet Infect. Dis. 2012;12:36–44.
[3] Fredriksen AB, Sandlie I, Bogen B. DNA vaccines increase immunogenicity of idiotypic tumor antigen by targeting novel fusion proteins to antigen-presenting cells. Mol. Ther. 2006;13:776–85.
[4] Grodeland G, Mjaaland S, Roux KH, Fredriksen AB, Bogen B. DNA vaccine that targets hemagglutinin to MHC class II molecules rapidly induces antibody-mediated protection against influenza. J. Immunol. 2013;191:3221–31.
[5] Carayanniotis G, Barber BH. Adjuvant-free IgG responses induced with antigen coupled to antibodies against class II MHC. Nature 1987;327:59–61.
[6] Kawamura H, Berzofsky JA. Enhancement of antigenic potency in vitro and immunogenicity in vivo by coupling the antigen to anti-immunoglobulin. J. Immunol. 1986;136:58–65.
[7] Snider DP, Segal DM. Targeted antigen presentation using crosslinked antibody heteroaggregates. J. Immunol. 1987;139:1609–16.
[8] Fredriksen AB, Bogen B. Chemokine-idiotype fusion DNA vaccines are potentiated by bivalency and xenogeneic sequences. Blood 2007;110:1797–805.
[9] Grodeland G, Fredriksen AB, Loset GA, Vikse E, Fugger L, Bogen B. Antigen Targeting to Human HLA Class II Molecules Increases Efficacy of DNA Vaccination. J. Immunol. 2016;197:3575–85.
[10] Rivera-Hernandez T, Carnathan DG, Moyle PM, Toth I, West NP, Young PR, et al. The contribution of non-human primate models to the development of human vaccines. Discov. Med. 2014;18:313–22.
[11] Thompson EA, Lore K. Non-human primates as a model for understanding the mechanism of action of toll-like receptor-based vaccine adjuvants. Curr. Opin. Immunol. 2017;47:1–7.
[12] Engelke L, Winter G, Hook S, Engert J. Recent insights into cutaneous immunization: How to vaccinate via the skin. Vaccine 2015;33:4663–74.
[13] Ledgerwood JE, Hu Z, Costner P, Yamshchikov G, Enama ME, Plummer S, et al. Phase I clinical evaluation of seasonal Influenza Hemagglutinin (HA) DNA vaccine prime followed by trivalent influenza inactivated vaccine (IIV3) boost. Contemp. Clin. Trials 2015.
[14] McAllister L, Anderson J, Werth K, Cho I, Copeland K, Le Cam BN, et al. Needle-free jet injection for administration of influenza vaccine: a randomised non-inferiority trial. Lancet 2014;384:674–81.
[15] Safronetz D, Rockx B, Feldmann F, Belisle SE, Palermo RE, Brining D, et al. Pandemic swine-origin H1N1 influenza A virus isolates show heterogeneous virulence in macaques. J. Virol. 2011;85:1214–23.
[16] Koopman G, Mooij P, Dekking L, Mortier D, Nieuwenhuis IG, van HM, Kuipers H, Remarque EJ, Radosevic K, Bogers WM. Correlation between virus replication and antibody responses in macaques following infection with pandemic influenza A virus. J. Virol. 2016;90:1023–33.
[17] Mooij P, Koopman G, Mortier D, van HM, Oostermeijer H, Fagrouch Z, de LR, Kobinger G, Li Y, Remarque EJ, Kondova I, Verschoor EJ, Bogers WM. Pandemic swine-origin H1N1 influenza virus replicates to higher levels and induces more fever and acute inflammatory cytokines in cynomolgus versus rhesus monkeys and can replicate in common marmosets. PLoS. One 2015;10:e0126132.
[18] Poon LL, Chan KH, Smith GJ, Leung CS, Guan Y, Yuen KY, et al. Molecular detection of a novel human influenza (H1N1) of pandemic potential by conventional and real-time quantitative RT-PCR assays. Clin. Chem. 2009;55:1555–8.
[19] McClain MT, Henao R, Williams J, Nicholson B, Veldman T, Hudson L, et al. Differential evolution of peripheral cytokine levels in symptomatic and asymptomatic responses to experimental influenza virus challenge. Clin. Exp. Immunol. 2016;183:441–51.
[20] Nickoloff BJ, Turka LA. Immunological functions of non-professional antigen-presenting cells: new insights from studies of T-cell interactions with keratinocytes. Immunol. Today 1994;15:464–9.
[21] Kim BS, Miyagawa F, Cho YH, Bennett CL, Clausen BE, Katz SI. Keratinocytes function as accessory cells for presentation of endogenous antigen expressed in the epidermis. J. Invest Dermatol. 2009;129:2805–17.
[22] Black AP, Ardern-Jones MR, Kasprowicz V, Bowness P, Jones L, Bailey AS, et al. Human keratinocyte induction of rapid effector function in antigen-specific memory $CD4^+$ and $CD8^+$ T cells. Eur. J. Immunol. 2007;37:1485–93.
[23] Slukvin II, Watkins DI, Golos TG. Phenotypic and functional characterization of rhesus monkey decidual lymphocytes: rhesus decidual large granular lymphocytes express CD56 and have cytolytic activity. J. Reprod. Immunol. 2001;50:57–79.

[24] Kuroda MJ, Schmitz JE, Charini WA, Nickerson CE, Lord CI, Forman MA, et al. Comparative analysis of cytotoxic T lymphocytes in lymph nodes and peripheral blood of simian immunodeficiency virus-infected rhesus monkeys. J. Virol. 1999;73:1573–9.
[25] Slierendregt BL, Otting N, van BN, Jonker M, Bontrop RE. Expansion and contraction of rhesus macaque DRB regions by duplication and deletion. J. Immunol. 1994;152:2298–307.
[26] Daza-Vamenta R, Glusman G, Rowen L, Guthrie B, Geraghty DE. Genetic divergence of the rhesus macaque major histocompatibility complex. Genome Res. 2004;14:1501–15.
[27] Daniel S, Caillat-Zucman S, Hammer J, Bach JF, van Endert PM. Absence of functional relevance of human transporter associated with antigen processing polymorphism for peptide selection. J. Immunol. 1997;159:2350–7.
[28] Grodeland G, Mjaaland S, Tunheim G, Fredriksen AB, Bogen B. The specificity of targeted vaccines for APC surface molecules influences the immune response phenotype. PLoS. One 2013;8:e80008.
[29] Fossum E, Grodeland G, Terhorst D, Tveita AA, Vikse E, Mjaaland S, et al. Vaccine molecules targeting Xcr1 on cross-presenting DCs induce protective $CD8^+$ T-cell responses against influenza virus. Eur. J. Immunol. 2015;45:624–35.
[30] Liang F, Lindgren G, Lin A, Thompson EA, Ols S, Rohss J, et al. Efficient targeting and activation of antigen-presenting cells in vivo after modified mRNA vaccine administration in rhesus macaques. Mol. Ther. 2017;25:2635–47.
[31] Loudon PT, Yager EJ, Lynch DT, Narendran A, Stagnar C, Franchini AM, et al. GM-CSF increases mucosal and systemic immunogenicity of an H1N1 influenza DNA vaccine administered into the epidermis of non-human primates. PLoS. One 2010;5:e11021.
[32] Koday MT, Leonard JA, Munson P, Forero A, Koday M, Bratt DL, et al. Multigenic DNA vaccine induces protective cross-reactive T cell responses against heterologous influenza virus in nonhuman primates. PLoS. One 2017;12:e0189780.
[33] Laddy DJ, Yan J, Khan AS, Andersen H, Cohn A, Greenhouse J, et al. Electroporation of synthetic DNA antigens offers protection in nonhuman primates challenged with highly pathogenic avian influenza virus. J. Virol. 2009;83:4624–30.
[34] Peng B, Zhao Y, Xu L, Xu Y. Electric pulses applied prior to intramuscular DNA vaccination greatly improve the vaccine immunogenicity. Vaccine 2007;25:2064–73.
[35] Lovas TO, Bruusgaard JC, Oynebraten I, Gundersen K, Bogen B. DNA vaccines: MHC II-targeted vaccine protein produced by transfected muscle fibres induces a local inflammatory cell infiltrate in mice. PLoS. One 2014;9:e108069.